the plant journal

SEB Society for Experimental Biology

The Plant Journal (2013) **73,** 733–746 doi: 10.1111/tpj.12060

The *Arabidopsis cer26* mutant, like the *cer2* mutant, is specifically affected in the very long chain fatty acid elongation process

Stéphanie Pascal[1,2,†], Amélie Bernard[1,2,†], Maud Sorel[1,2,†], Marjorie Pervent[3], Denis Vile[3], Richard P. Haslam[4], Johnathan A. Napier[4], René Lessire[1,2], Frédéric Domergue[1,2] and Jérôme Joubès[1,2,*]

[1]*Laboratoire de Biogenèse Membranaire, Université de Bordeaux, UMR5200, F-33000 Bordeaux, France,*

[2]*Laboratoire de Biogenèse Membranaire, CNRS, UMR5200, F-33000 Bordeaux, France,*

[3]*LEPSE, UMR759, INRA-SupAgro, F-34060 Montpellier, France, and*

[4]*Rothamsted Research, Harpenden, Herts AL5 2JQ, UK*

Received 23 July 2012; revised 15 October 2012; accepted 19 October 2012; published online 13 February 2013.

*For correspondence (e-mail jjoubes@biomemb.u-bordeaux2.fr).

†These authors contributed equally to this work.

The author responsible for distribution of materials integral to the findings presented in this article in accordance with the policy described in the Instructions for Authors (http://mc.manuscriptcentral.com/tpj) is Jérôme Joubès (jjoubes@biomemb.u-bordeaux2.fr).

SUMMARY

Plant aerial organs are covered by cuticular waxes, which form a hydrophobic crystal layer that mainly serves as a waterproof barrier. Cuticular wax is a complex mixture of very long chain lipids deriving from fatty acids, predominantly of chain lengths from 26 to 34 carbons, which result from acyl-CoA elongase activity. The biochemical mechanism of elongation is well characterized; however, little is known about the specific proteins involved in the elongation of compounds with more than 26 carbons available as precursors of wax synthesis. In this context, we characterized the three Arabidopsis genes of the CER2-like family: *CER2*, *CER26* and *CER26-like* . Expression pattern analysis showed that the three genes are differentially expressed in an organ- and tissue-specific manner. Using individual T–DNA insertion mutants, together with a *cer2 cer26* double mutant, we characterized the specific impact of the inactivation of the different genes on cuticular waxes. In particular, whereas the *cer2* mutation impaired the production of wax components longer than 28 carbons, the *cer26* mutant was found to be affected in the production of wax components longer than 30 carbons. The analysis of the acyl-CoA pool in the respective transgenic lines confirmed that inactivation of both genes specifically affects the fatty acid elongation process beyond 26 carbons. Furthermore, ectopic expression of CER26 in transgenic plants demonstrates that CER26 facilitates the elongation of the very long chain fatty acids of 30 carbons or more, with high tissular and substrate specificity.

Keywords: cuticle, waxes, very long chain fatty acids, *cer2*, *cer26*, *Arabidopsis thaliana*.

INTRODUCTION

Terrestrial plants have developed a protective barrier, or cuticle, that controls the movement of water between the outer cell wall of the epidermis and the atmosphere adjacent to the plant (Shepherd and Wynne Griffiths, 2006). The cuticle is a rather thin membrane consisting of cutin, polysaccharides and associated solvent-soluble lipids, called cuticular waxes. Cutin is the main structural component of the cuticular matrix. It consists of a three-dimensional polymer of mostly C16 and C18 hydroxy fatty acids cross-linked by ester bonds (Beisson *et al.*, 2012). Cuticular waxes are a complex mixture of very long chain (VLC) aliphatic lipids, triterpenoids and minor secondary metabolites, such as sterols and flavonoids (Buschhaus and Jetter, 2011). The physical and chemical properties of cuticular waxes determine vital functions for plants (Dominguez *et al.*, 2011). Indeed, besides playing a major role in limiting uncontrolled water loss (Kosma *et al.*, 2009), waxes protect plants against ultraviolet radiation and help to minimize deposits of dust, pollen and air pollutants (Kunst and Samuels, 2003). In addition, surface wax is believed to play important roles in plant defense against bacterial and fungal pathogens (Raffaele *et al.*, 2009), and has been shown to participate in a variety of plant–insect interactions (Eigenbrode *et al.*, 2000).

Wax aliphatic compounds are produced in epidermal cells via two different pathways: the alcohol-forming pathway, which produces VLC alcohols and esters (Rowland *et al.*, 2006; Li *et al.*, 2008), and the alkane-forming pathway leading to the formation of VLC alkanes and their derivatives (Greer *et al.*, 2007; Bernard *et al.*, 2012). The two metabolic routes share a pool of precursors consisting of VLC fatty acids (VLCFAs), with predominant chain lengths ranging from 26 to 34 carbons. VLCFAs result from the endoplasmic reticulum (ER)-associated acyl-CoA elongase activity, which is carried out by multi-enzymatic fatty acid elongase (FAE) complexes (von Wettstein-Knowles, 1982). Each elongation cycle catalyzes four successive reactions, generating an acyl chain extended by two carbons. The first step of elongation, which consists of the condensation of an acyl-CoA with a malonyl-CoA, is catalyzed by 3–ketoacyl-CoA synthase (KCS). The resulting 3–ketoacyl-CoA is then reduced by 3–ketoacyl-CoA reductase (KCR) into 3–hydroxyacyl-CoA, which is subsequently dehydrated by 3–hydroxacyl-CoA dehydratase (HCD) to form a *trans*-2,3-enoyl-CoA. In the final elongation step, the *trans*-2,3-enoyl-CoA is reduced by the *trans*-2,3-enoyl-CoA reductase (ECR), which yields an acyl-CoA elongated by two carbons. In plants, evidence suggests that multiple elongases with distinct chain-length specificity are likely to exist, producing the broad range in chain lengths of VLCFAs (von Wettstein-Knowles, 1982). The KCR, HCD and ECR enzymes are thought to have broad substrate specificity and to be shared by all FAE complexes (Kunst and Samuels, 2009). In contrast, KCS enzymes have been proposed to determine the chain length substrate specificity of each elongation reaction. Consistently, 21 putative *KCS* have been annotated in the Arabidopsis genome (Joubès *et al.*, 2008), but to date only a few of them have been characterized in depth. In particular, although wax component chain lengths vary from C22 to C34, suggesting that VLCFA precursors would result from various elongase complexes, only four KCS (FDH, KCS1, HIC and CER6) with a potential role in wax precursor synthesis have been identified and analyzed in detail (Yephremov *et al.*, 1999; Todd *et al.*, 1999; Millar *et al.*, 1999; Pruitt *et al.*, 2000; Gray *et al.*, 2000). Notably, based on expression patterns, mutant phenotypes and heterologous expression in yeast, *CER6* was shown to have a major role in the production of fatty acids with 26 and 28 carbons (Millar *et al.*, 1999; Fiebig *et al.*, 2000; Tresch *et al.*, 2012). Similar to the *cer6* mutant, the Arabidopsis *cer2* mutant shows a defect in all classes of wax compounds causing a 40% reduction of the total quantity of stem waxes compared with wild-type plants (Hannoufa *et al.*, 1993). All components with more than 28 carbons were found to be depleted in the *cer2* mutant, whereas compounds with 28 or less carbons were consistently over-accumulated, suggesting a block in the elongation of C28 VLCFAs. Based on these observations it has been proposed that *CER2* encodes a component of the elongase (McNevin *et al.*, 1993). Nevertheless, CER2 does not share sequence similarities with any of the elongase enzymes, suggesting that CER2 could instead function as a regulator of the elongase system specific for the last elongation steps (Jenks *et al.*, 1995). CER2 was previously reported as being localized in the nucleus based on immunodetection using subcellular fractions, which would be consistent with a regulatory role (Xia *et al.*, 1997); however, latterly it has been shown that CER2 is localized in the ER of young stem epidermal cells, i.e. at the site of VLCFA biosynthesis, thereby supporting the hypothesis of its role as a component of the elongase complex (Haslam *et al.*, 2012). Finally, evidence has been provided for the role of CER2 in C28 elongation, as the co-expression of CER2 with CER6 in yeast resulted in the production of C30 fatty acids (Haslam *et al.*, 2012).

Although *CER2* is expressed in all aerial organs in Arabidopsis, the *cer2* mutation does not affect leaf wax composition (Jenks *et al.*, 1995; Negruk *et al.*, 1996; Xia *et al.*, 1996), suggesting that other proteins could be involved in VLCFA elongation in leaves. CER2 is a member of the BAHD superfamily of acyl-CoA-dependent acyltransferases, and clusters in group V with two other proteins, At4g13840 (herein called CER26, which shows 32.2% identity with CER2) and its close homologue At3g23840 (herein called CER26-like, which shows 35.7% identity with CER2 and 64% identity with CER26; Figure S1; Yu *et al.*, 2009). In order to better understand the elongation process leading to the formation of VLC wax precursors in leaves, the CER2-like family members were characterized here. A detailed molecular analysis showed that *CER2* and *CER26* have overlapping expression patterns in leaves, whereas *CER26* expression is excluded from the stem. Insertional mutants for each of the three genes and *CER26* overexpressing lines were identified and characterized at the biochemical level, showing that CER26 is involved in the elongation of VLCFAs longer than 30 carbons, and has overlapping function with CER2 in leaves. Altogether, our results demonstrate that CER26, like CER2, is involved in the formation of VLC fatty acids, and support its role as an element of the fatty acid elongation machinery for wax synthesis.

RESULTS

Expression profiling in Arabidopsis organs of the *CER2*-like genes

The organ distribution of *CER2*, *CER26* and *CER26-like* was determined by real-time PCR in seedlings, roots, stems, cauline and rosette leaves, flowers and siliques (Figure 1a). The three genes showed a typical wax-associated expression pattern, as they were found expressed in aerial vegetative and reproductive organs, but not in roots. *CER2* was

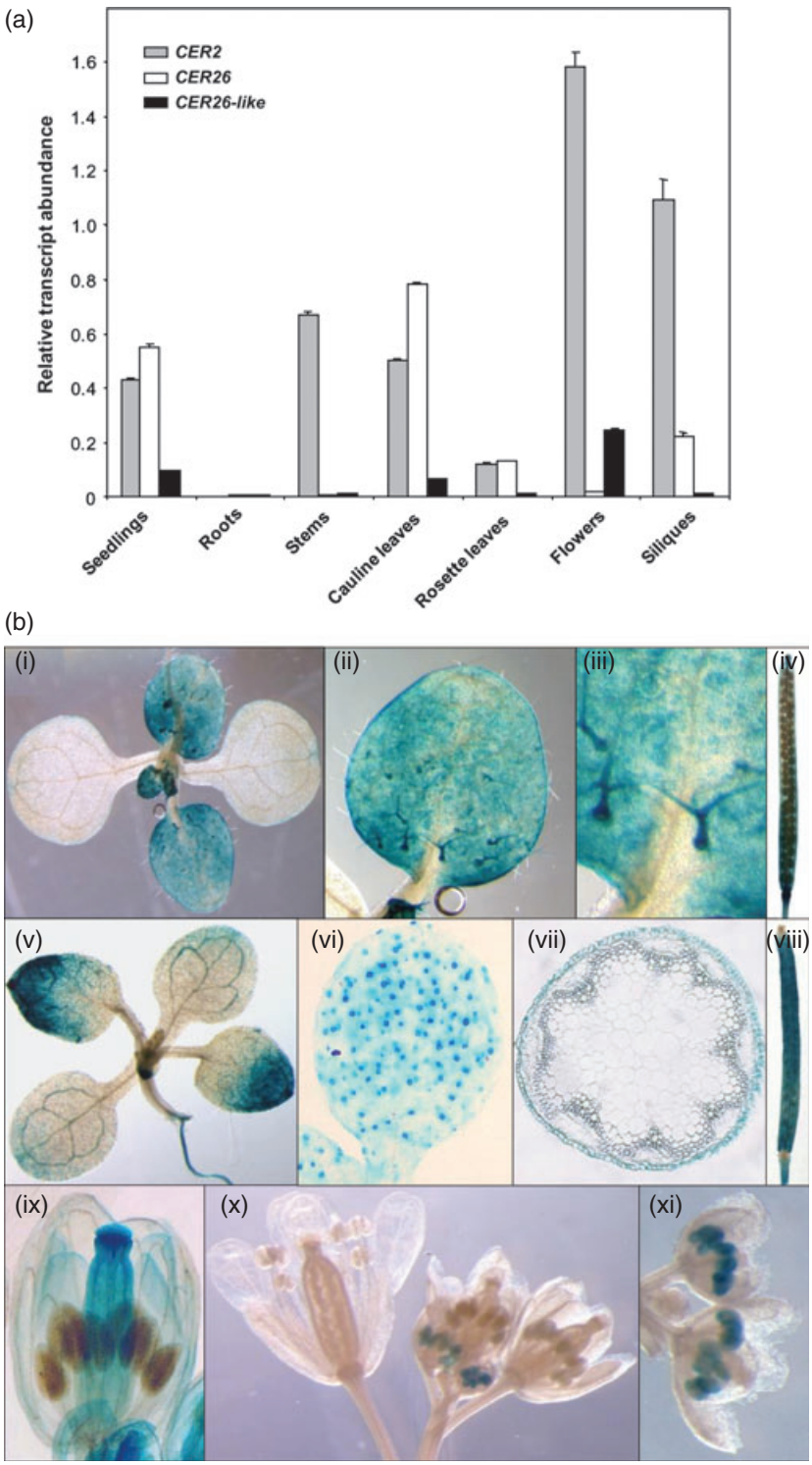

Figure 1. Expression analysis of the *CER2-like* gene family in Arabidopsis.
(a) Differential expression analysis of Arabidopsis *CER2, CER26 and CER26*-like genes in various organs of Arabidopsis. The gene expression level was determined by real-time RT-PCR analysis. Results are presented as relative transcript abundances. The data represent the means ± SDs of five replicates. Total RNA was isolated from 15–day-old seedlings, roots, stems, cauline leaves, rosette leaves, flowers and siliques.
(b) Spatial expression patterns of the *CER26* (i, ii, iii, iv), *CER2* (v, vi, vii, viii, ix) *and CER26*-like (x, xi) genes in transgenic Arabidopsis plants harboring the *CER2, CER26 and CER26*-like promoters fused to the *GUS* gene. Promoter activity was visualized through histochemical GUS staining on (i, v) 10–day-old plants, (ii, iii, vi) young leaves of 10–day-old plants, (vii) transverse section of the stem, (iv, viii) young siliques, (ix, x, xi) flowers.

expressed in all aerial organs, and it was notably the only gene of the cluster expressed in stems. Indeed, compared with *CER2*, *CER26* was found highly expressed in leaves, but no transcripts were detected in stems. Furthermore, *CER26* was weakly expressed in flowers and siliques. *CER26-like* was mainly expressed in flowers and expressed at very low levels in all other tissues. These results are in agreement with microarray data available in the Genevestigator gene expression database (http://www.genevestigator.ethz.ch).

To investigate the cell-type expression pattern of the three genes, we generated transgenic Arabidopsis lines expressing the *β–glucuronidase* (*GUS*) reporter gene under the control of each of the three promoter sequences (Figure 1b). Several homozygous reporter lines showed a similar expression pattern, which was consistent with real-time reverse transcription (RT)-mediated PCR analysis. In young leaves, *CER26* expression was detected in epidermal cells and trichomes (Figure 1b). Under the control of the *CER2* promoter, GUS expression was detected in leaf epidermal cells and the signal was also specifically localized in the guard cells (Figure 1b). *CER2* expression was detected specifically in the epidermis of the elongated floral stems (Figure 1b). Both *CER26* and *CER2* promoter activities were detected in siliques, where the expression of *CER26* was found mostly expressed in the pod dehiscence zones, whereas *CER2* was localized in the pod epidermis (Figure 1b). In young flowers, *CER2* promoter activity was detected in the pistil, the petals and the sepals (Figure 1b). *CER26-like* promoter activity was only detected in stamens at early stages of flower development (Figure 1b). These results show that *CER2*, *CER26* and *CER26-like* are differentially expressed at the tissue and organ level throughout plant development, suggesting that they could perform different or complementary functions in wax biosynthesis.

Molecular identification of Arabidopsis mutants

To understand the role of the CER2-like proteins in the production of cuticular waxes, we selected the *cer26* allele (SALK_087857 in the Col–0 ecotype), in which the *CER26* gene was disrupted in the intronic region (at nucleotide 480 relative to the start codon) (Figure 2a). We also identified a *cer26-like* mutant (SAIL_3_F11 in the Col–0 ecotype), which showed a T–DNA insertion in the first exon of the gene (at nucleotide 200 relative to the start codon). As previously reported, *cer2* mutants were in the genetic background *Ler*–0 (Koornneef *et al.*, 1989) or WS (McNevin *et al.*, 1993), and we selected the insertional *cer2* mutant (SALK_0844439) in the Arabidopsis ecotype Col–0 for comparison with *cer26* and *cer26-like* mutants (Figure 2a). The T–DNA insertion in *cer2* disrupted the second exon of the *CER2* gene (at nucleotide 814 relative to the start codon). The T–DNA insertions were confirmed by PCR on genomic DNA (Figure 2b). Given that *CER2* and *CER26* have overlapping expression pattern in leaves, we hypothesized that the absence of any wax phenotype in leaves of the *cer2* mutant could result from a potential compensatory function of *CER26*. To test this hypothesis we further generated a *cer2 cer26* double mutant by crossing the *cer2* and *cer26* lines. Gene expression was analyzed by semi-quantitative RT-PCR in leaves and stems of the *cer2*, *cer26* and *cer2 cer26* mutants, and in flower transcripts for the *cer26-like* line (Figure 2c). No corresponding full-length transcripts were detected in the different alleles. This observation was confirmed by qRT–PCR in vegetative or reproductive organs of the different single mutants and the *cer2 cer26* double mutant (Figure 2d). It is worth noting that the absence of expression of *CER2*, *CER26, CER26-like* or both *CER2* and *CER26* did not lead to compensatory overexpression of the remaining members of the gene family in the single or double mutants (Figure 2d).

The *cer2* and *cer2 cer26* mutants only show glossy stems

To define the growth characteristics of the different lines, the plants were cultivated in the automated phenotyping platform PHENOPSIS, which was designed for the strict control of environmental conditions (Granier *et al.*, 2006). Wild-type (Col–0), *cer2, cer26* and *cer2 cer26* growth was phenotyped by measuring several morphological and anatomical traits in optimal plant growth conditions (Table S1). When compared with the wild-type line, the *cer2, cer26* and *cer2 cer26* mutants did not show significantly different leaf growth variables, i.e. rosette leaf number, rosette leaf area, and the area and thickness of leaf 6. Moreover, fresh and dry weights of rosettes at bolting were not significantly modified compared with those of wild-type rosettes. A detailed analysis of epidermal cells on the adaxial side of leaf 6 in *cer2, cer26* and *cer2 cer26* mutants, compared with wild-type plants, did not reveal any differences. The *cer2, cer26* and *cer2 cer26* lines were similar in all aspects to wild-type plants (Figure 3a), except for the bright-green stem phenotype exhibited by the *cer2* and *cer2 cer26* mutants (Figure 3b). This phenotype, typically associated with wax-deficient mutants, indicates qualitative and/or quantitative modifications in the production of cuticular waxes on the stem surface. These observations were confirmed by scanning electron microscopy analysis of young stem surfaces of wild-type, *cer2, cer26* and *cer2 cer26* lines (Figure 3c). The *CER2* inactivation in *cer2* and *cer2 cer26* lines led to the complete disappearance of the wax crystals formed on the stem surface, whereas the stem surface of the *cer26* line was similar to that of wild-type plants.

Arabidopsis *cer2* and *cer26* mutants show altered cuticular wax composition

In order to assess the deregulating effect of *CER2*, *CER26* and *CER26-like* expression on cuticular waxes, the cuticular

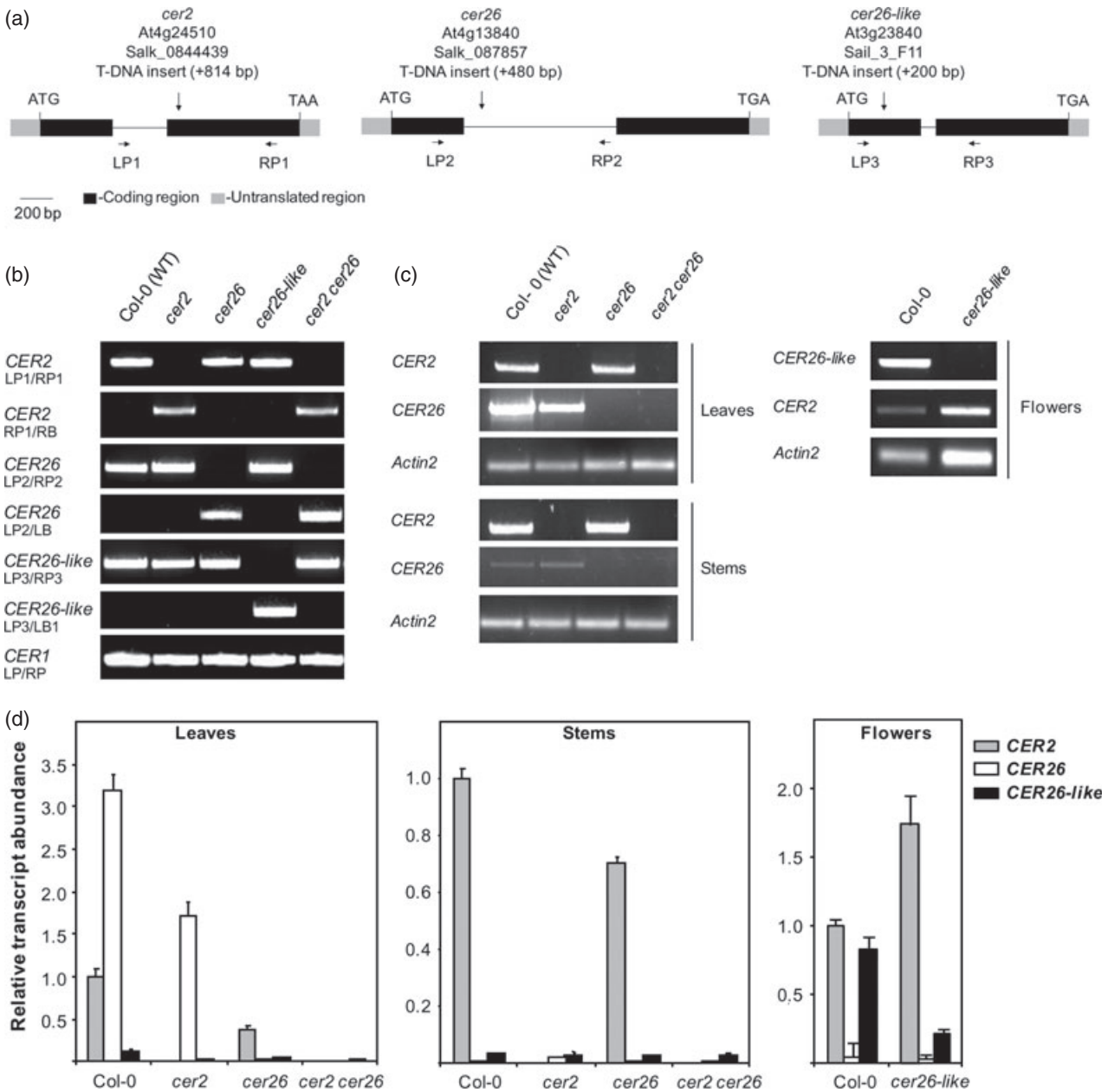

Figure 2. Molecular characterization of *cer2, cer26 and cer26-like* single mutants and the *cer2 cer26* double mutant.
(a) Schematic of *CER2, CER26* and *CER26-like* gene structure, indicating the positions of the T–DNA inserts in the mutant alleles. Dark boxes indicate exons, black lines indicate introns, and grey boxes indicate 5′- and 3′-untranslated regions. The arrows underneath the gene structure are the positions of convergent primers used for PCR on genomic DNA.
(b) PCR on genomic DNA of wild-type (Col–0) plants, *cer2, cer26, cer26-like* and *cer2 cer26* mutants. Amplification of the *CER1* gene was used as a positive control.
(c) Semi-quantitative RT-PCR analysis of steady-state *CER2, CER26* and *CER26-like* transcripts in leaves, stems or flowers of the different lines, compared with the wild-type plants, as indicated above. The *Actin2* gene was used as a constitutively expressed control.
(d) Real-time RT-PCR analysis of *CER2, CER26* and *CER26-like* gene expression in leaves, stems or flowers of the different lines, compared with wild-type plants, as indicated above. Results are presented as relative transcript abundances. The data represent the means ± SDs of three replicates.

wax composition of stems and leaves of the different lines: Col–0 (wild type, WT), *cer2*, *cer26*, *cer26-like* and *cer2 cer26* was analyzed in detail (Figures 4 and S2; Tables 1 and 2).

In stems, the wax load of *cer2* and *cer2 cer26* was strongly reduced compared with wild-type plants (an average 38% decrease), whereas neither the wax load nor the wax composition of *cer26* was significantly affected (Figure 4; Table 1). The decrease measured in *cer2* and *cer2 cer26* was largely the result of reduced levels in the three major components of stem waxes: the C29 alkane and its derivatives C29 2°–alcohol and C29 ketone. The *CER2* inactivation further affected all wax components according to a

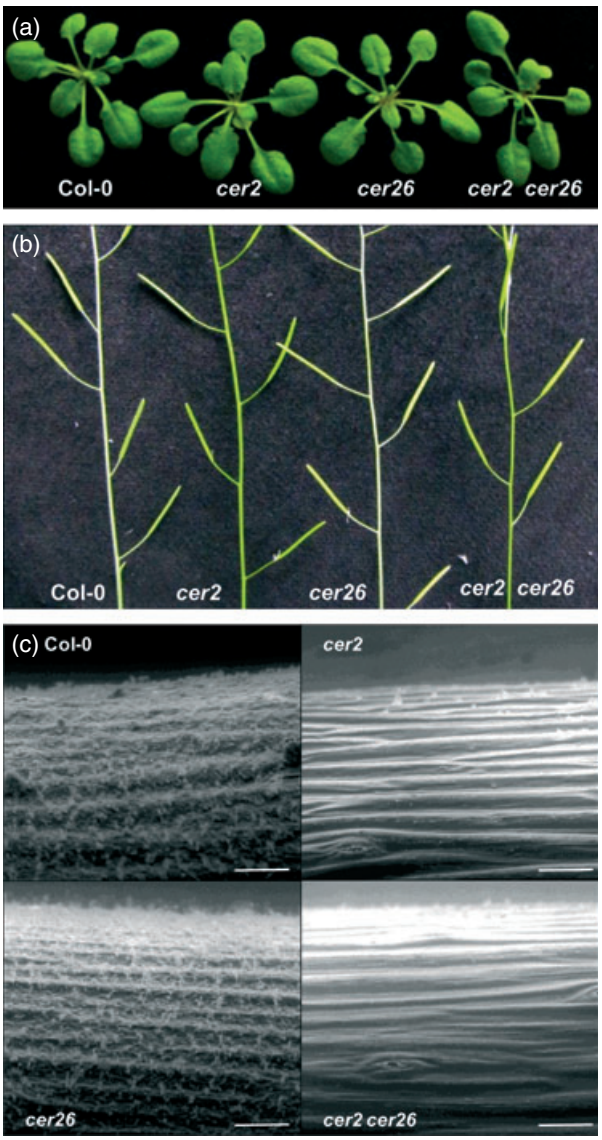

Figure 3. Phenotypes of *cer2, cer26* and *cer2 cer26* mutants.
(a) Phenotype of 4–week-old rosettes of Col–0 (WT), *cer2*, *cer26* and *cer2 cer26* lines.
(b) Stems from 6–week-old *cer2* and *cer2 cer26* mutants showing glossy phenotypes compared with the stems of wild-type and *cer26* plants.
(c) Epicuticular wax crystal visualization on Arabidopsis wild-type (Col–0), *cer2*, *cer26* and *cer2 cer26* stem surfaces detected by ESEM at 2800× magnification. Scale bars: 20 μm.

specific carbon chain length. Indeed, the level of components with more than 28 carbons was dramatically decreased (C31 alkane, C30 1°–alcohol, C30 aldehyde), whereas the level of components with 28 or less carbons was increased (C27 alkane, C27 2°–alcohol, C26 and C28 1°–alcohols, C26 and C28 aldehydes, C26 and C28 VLCFAs), together with the level of C42 and C44 esters, which contain C26 and C28 esterified alcohols. In accordance with previous studies of *cer2* mutants (Jenks *et al.*, 1995; Negruk *et al.*, 1996; Xia *et al.*, 1996; Haslam *et al.*, 2012), these results suggest that a defective CER2 blocks the formation of wax compounds with more than 28 carbons in stems.

In leaves, the wax load of the single *cer2* and *cer26* mutants was almost not affected when compared with wild-type plants (Table 2), whereas the wax load of the double *cer2 cer26* mutant was considerably reduced (43% decreased). Whereas the wax profile of *cer2* was comparable with that of the wild-type plants, the wax composition of *cer26* was substantially modified (Figure 4; Table 1). The level of components with 30 or less carbons was increased (C29 alkane, C30 aldehyde, C30 VLCFA and C30 1°–alcohol), whereas the level of components with more than 30 carbons was decreased (C31, C33 and C35 alkanes, C32 aldehyde, and C32 1°–alcohol), suggesting a block in the synthesis of wax components with more than 30 carbon atoms. Because of this modified wax profile, the mutant can be associated with the large family of *eceriferum* (*cer*) mutants that are characterized by a modification of the quantity and/or quality of epicuticular waxes onto stems or leaves. To date, 25 *eceriferum* mutants have been described (Rashotte *et al.*, 2004; Goodwin *et al.*, 2004), and therefore we named this new mutant *cer26*.

The double *cer2 cer26* mutant showed a novel wax phenotype. The level of components with more than 28 carbons was largely reduced (C29, C31, C33 and C35 alkanes, C30 VLCFAs, C30 and C32 1°–alcohols, C30 and C32 aldehydes), whereas the level of components with 28 or less carbon atoms was increased (C27 alkane, C28 1°–alcohol, C28 aldehyde, C28 VLCFA). These results demonstrate a role for CER2 in the formation of wax compounds with more than 28 carbons, and suggest that CER26 could compensate for the loss of CER2 activity in *cer2* leaves.

The inactivation of *CER26-like* did not lead to any modification in the wax composition of stems, leaves or even flowers in which the gene is specifically expressed (Figure S2). Therefore, the *CER26-like* gene was not further characterized.

Ectopic expression of *CER26* in the stem altered cuticular wax organization

To further understand CER26 function in wax metabolism, the *cer26* allele was complemented with a construct harboring the *CER26* gene under the control of *Pro35S* and, among several obtained lines that showed a similar phenotype, one line was selected for deeper analysis (*cer26R*). T–DNA insertions were confirmed by PCR on genomic DNA (Figure 5a), and gene expression was analyzed by qRT-PCR in leaves (Figure 5b). No transcripts were detected in *cer26* compared with wild-type plants, whereas the rescued *cer26* line exhibited a *CER26* transcript level almost similar to that of wild-type plants.

The cuticular wax composition was determined in the stems and leaves of the different lines: Col–0 (WT), *cer26*

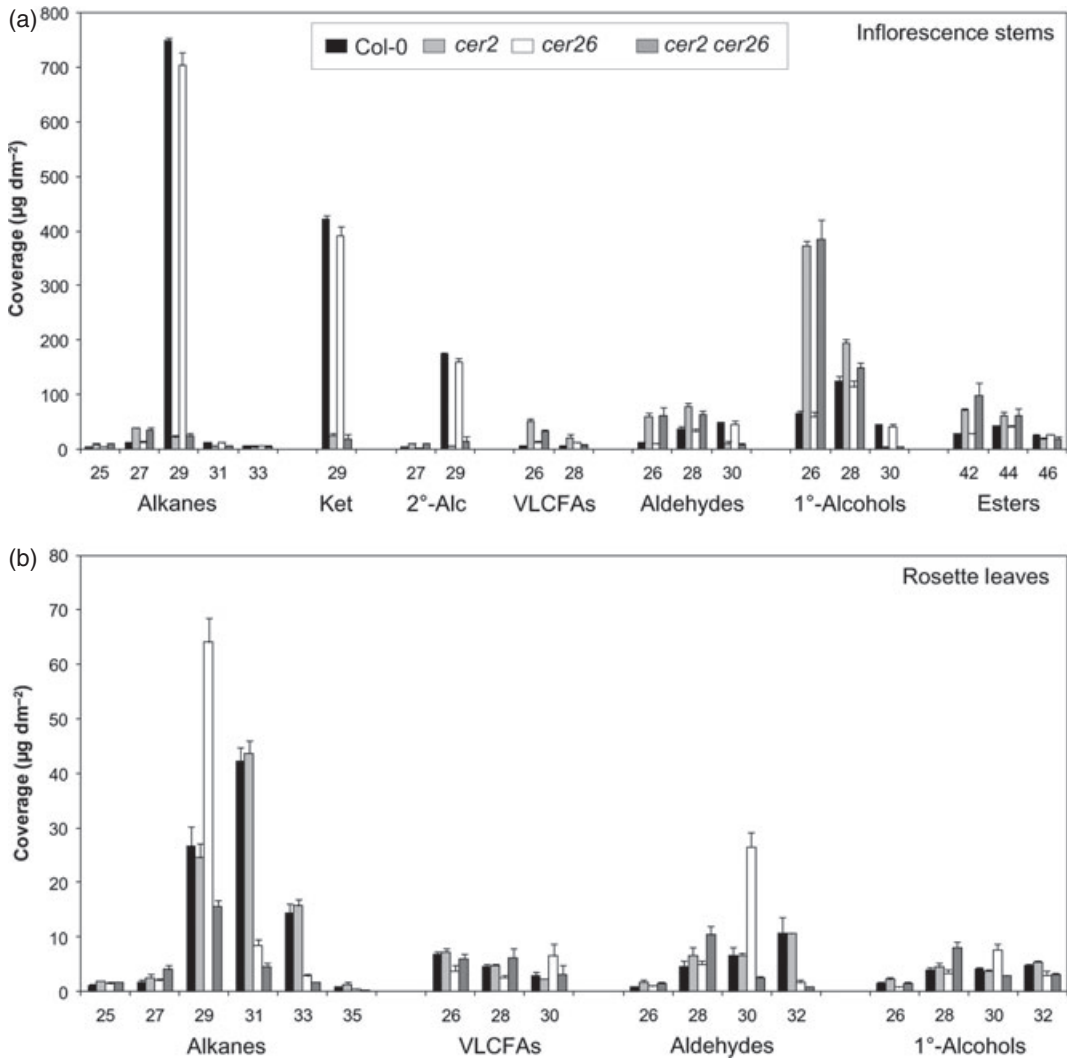

Figure 4. Cuticular wax composition of *cer2*, *cer26* and *cer2 cer26* mutants.
(a) Cuticular wax composition on inflorescence stems of Col–0 (WT), *cer2*, *cer26* and *cer2 cer26* lines.
(b) Cuticular wax composition on rosette leaves of Col–0 (WT), *cer2*, *cer26* and *cer2 cer26* lines. Levels of major components are expressed as µg dm^{-2} of stem or leaf surface area. Each wax constituent is designated by carbon chain length, and is labeled by chemical class along the *x*–axis (Ket, ketone; 2°–Alc, secondary alcohols; VLCFAs, very long chain fatty acids). The data represent means ± SDs of four replicates.

and *cer26R* (Figure 5c; Tables 1 and 2). *CER26* expression in the *cer26* background rescued the correct wax biosynthesis in leaves (Figure 5c; Table 2). Indeed, compared with the *cer26* mutant, the level of all compounds with 30 or less carbons (C29 alkane, C30 aldehyde and C30 1°–alcohol) was reduced, whereas the level of the components with more than 30 carbons was increased (C31, C33 and C35 alkanes, C32 aldehyde, and C32 1°–alcohol), thus confirming the role of CER26 in the elongation of VLCFAs longer than 30 carbons. *CER26* ectopic expression in stems reduced the wax load compared with wild-type plants (12% decreases; Table 1). This decrease was mainly caused by a slight reduction of the three major components of the stem waxes: C29 alkane, C29 2°–alcohol and C29 ketone (Figure 5c). Strikingly, the stems of the *CER26R* line showed a large increase of the C31 and C33 alkane levels compared with wild-type plants (increases of 1883 and 404%, respectively). This phenotype shows that ectopic expression of CER26 in stems leads to the production of components with more than 30 carbons, and therefore supports the hypothesis that CER26 could have a role in the elongation process of VLCFA with 30 or more carbon atoms.

Surprisingly, the *cer26R* line displays a bright-green stem phenotype (Figure 5d), which is usually associated with a depletion of wax crystals in *cer* mutants. In fact, scanning electron microscopy analyses showed that ectopic expression of *CER26* in stems induced the formation

Table 1 Cuticular wax composition of inflorescence stems of Arabidopsis Col–0 (WT), *cer2*, *cer26*, *cer2 cer26* and *cer26R*

	Total load	n-alkanes	2°-alcohols	Ketones	1°-alcohols	Iso-alcohols	Aldehydes	Esters	Fatty acids
Col-0	1 907.7 ± 82.4	815.6 ± 37.3	177.7 ± 7.9	421.9 ± 6.7	246.7 ± 7.6	10.9 ± 0.8	100.0 ± 30.3	20.4 ± 2.5	114.4 ± 4.9
cer2	1 182.8 ± 53.1	122.3 ± 11.9	15.2 ± 0.7	25.0 ± 4.0	583.6 ± 67.5	38.3 ± 6.2	154.0 ± 20.7	80.3 ± 10.0	164.1 ± 22.6
cer26	1 811.4 ± 53.1	776.9 ± 65.0	162.2 ± 11.5	391.6 ± 15.9	226.9 ± 15.4	14.4 ± 1.2	92.8 ± 11.9	30.0 ± 2.4	116.7 ± 10.1
cer2 cer26	1 108.9 ± 98.7	124.4 ± 20.5	21.8 ± 8.4	18.4 ± 9.5	546.4 ± 71.4	31.1 ± 2.9	124.5 ± 12.0	47.2 ± 6.7	195.2 ± 19.4
cer26R	1 686.3 ± 112.4	770.5 ± 69.5	135.3 ± 14.0	313.8 ± 9.7	228.4 ± 16.7	14.2 ± 4.7	41.5 ± 13.4	29.1 ± 6.0	153.4 ± 8.3

Mean values (μg dm^{-2}) of total wax loads and coverage of individual compound classes are given with SDs (n = 4). The sums include shorter chain length constituents not presented in Figures 4 and 5.

of an amorphous wax layer instead of the typical crystalline organization. As the total wax level of the *cer26R* line is only slightly reduced compared with the WT, we hypothesize that the change in the structure of waxes would result from the qualitative modification of the wax composition.

cer2 and *cer26* mutations specifically affect VLCFA-containing lipids

In plant cells, VLCFAs are used as precursors by multiple biochemical pathways leading to the formation of a wide variety of lipid molecules, such as phospholipids, sphingolipids, storage lipids, cutin, waxes and suberin. To further determine the role of CER2 and CER26 in VLCFA elongation, a global analysis of the VLCFA-containing lipids was performed in WT, *cer2*, *cer26* and *cer2 cer26* lines. The cutin polyester of stems and leaves from the different lines was extracted and depolymerized prior to the quantitative and qualitative analysis of cutin momoners. The different lines showed a similar cutin composition in both stem and leaf (Figure S3). Similarly, neither the suberin composition nor the seed lipid profile were found to be significantly affected in the different transgenic lines compared with the WT (Figures S4 and S5). Furthermore, the effect of *cer2* and *cer26* deregulation on the intracellular fatty acyl chain content was examined after the removal of the cuticular waxes of stems and leaves of the different lines. No modification of the general cellular fatty acyl chain profile was observed (Figure S6), except for slight modifications of the VLCFAs with chain length longer than 26 carbon atoms, which were in accordance with the changes observed in stem and leaf wax composition of the different transgenic lines.

Arabidopsis *cer2* and *cer26* mutants show altered acyl-CoA composition

The phenotype of *cer2*, *cer26* and *cer2 cer26* shows that the two proteins participate in the formation of VLC wax compounds, suggesting that they have a role in the terminal steps of fatty acid elongation. To test this hypothesis, the acyl-CoA pool of young stems and leaves of *cer2, cer26* and *cer2 cer26* lines was compared with the wild type (Figure 6). These analyses showed significant modifications of the acyl-CoA profiles, which were consistent with the changes observed in the wax profiles. Indeed, in stems both *cer2* and *cer2 cer26* acyl-CoA pools were affected (Figure 6a): the level of C26 acyl-CoA was largely increased, whereas C30 acyl-CoA was almost completely absent. Surprisingly, the level of C28 acyl-CoA was only slightly increased in the two lines compared with the WT. The acyl-CoA profile of *cer26* stems was not modified compared with the wild-type profile. In *cer2* rosette leaves, the acyl-CoA pool composition was not affected (Figure 6b). In rosette leaves of the *cer26* mutant, the profile showed a large increase of C30 acyl-CoA. The *cer2 cer26* double mutant showed a different profile, with a large increase of C28 acyl-CoA, accompanied by a slight reduction of C30 acyl-CoA. Collectively, these results demonstrate that *CER2* and *CER26* inactivation affects the VLCFA elongation process at specific stages.

Table 2 Cuticular wax composition of rosette leaves of Arabidopsis Col–0 (WT), *cer2*, *cer26*, *cer2 cer26* and *cer26R*

	Total load	n-alkanes	Iso-alkanes	1°-alcohols	Iso-alcohols	Aldehydes	Fatty acids	Esters
Col-0	162.3 ± 4.7	93.1 ± 3.5	3.2 ± 0.3	14.7 ± 1.1	9.9 ± 0.9	23.2 ± 2.0	16.1 ± 0.8	2.1 ± 0.2
cer2	172.3 ± 5.5	97.0 ± 4.2	3.5 ± 0.2	16.2 ± 2.0	9.9 ± 0.8	25.8 ± 1.6	16.2 ± 0.8	3.7 ± 0.5
cer26	162.1 ± 6.6	83.8 ± 5.4	2.8 ± 0.3	14.9 ± 1.7	10.9 ± 1.7	34.3 ± 3.3	13.9 ± 1.7	1.6 ± 0.1
cer2 cer26	92.6 ± 3.2	31.2 ± 1.4	2.7 ± 0.3	15.5 ± 0.8	9.4 ± 0.8	15.4 ± 1.2	16.5 ± 2.2	1.9 ± 0.2
cer26R	167.8 ± 4.8	98.2 ± 3.9	2.4 ± 0.3	14.3 ± 0.9	9.1 ± 0.4	24.0 ± 0.9	17.3 ± 1.7	2.7 ± 0.1

Mean values (μg dm^{-2}) of total wax loads and coverage of individual compound classes are given with SDs (n = 4). The sums include shorter chain length constituents not presented in Figures 4 and 5.

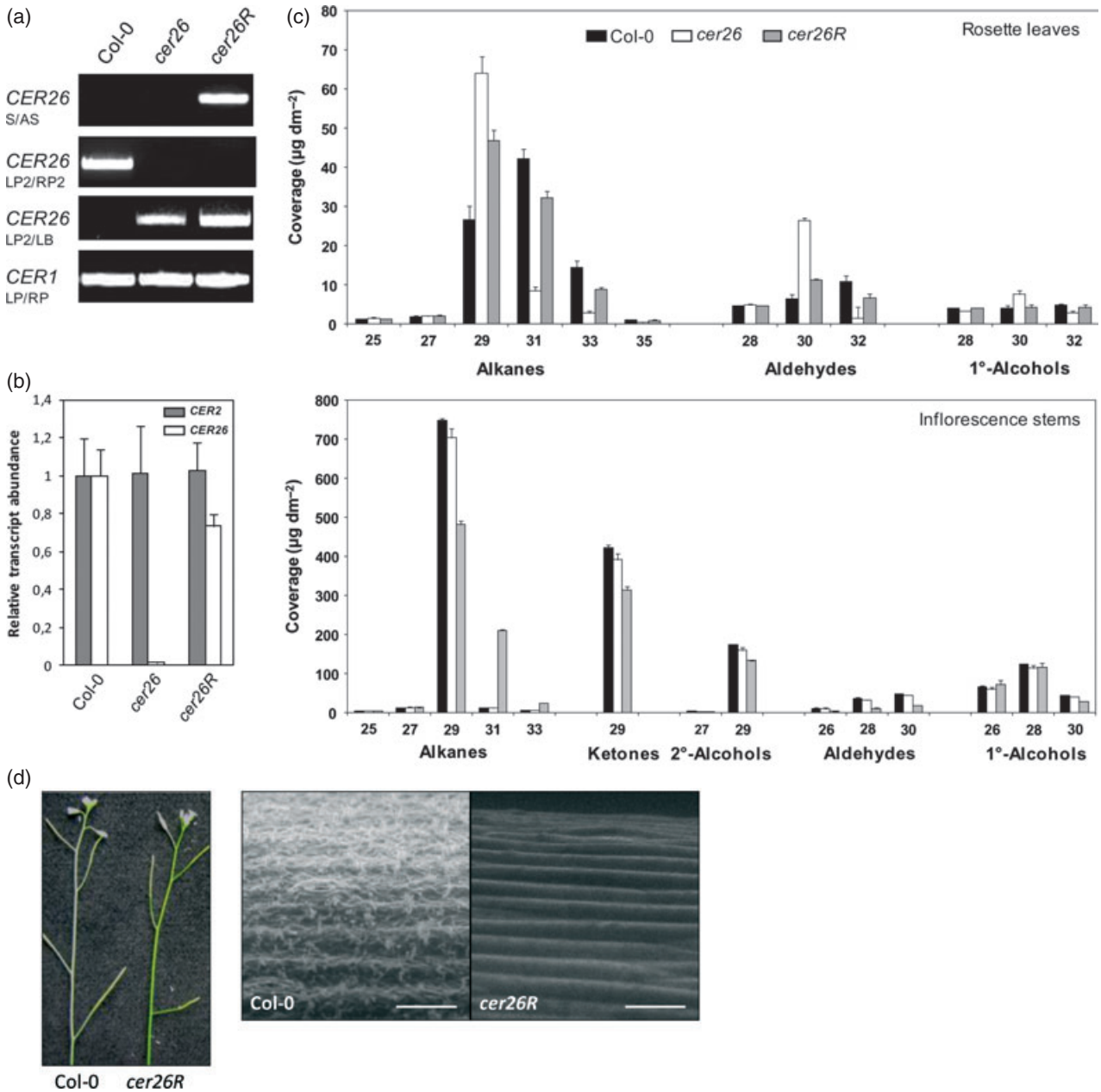

Figure 5. Molecular, biochemical and phenotypical characterization of *cer26R* transgenic plants.
(a) PCR on genomic DNA of wild-type (Col-0) plants, *cer26* mutant and the *cer26R* rescued line. Amplification of the *CER1* gene was used as a positive control.
(b) Real-time RT-PCR analysis of *CER2* and *CER26* gene expression in wild-type (Col–0), *cer26* and *cer26R* seedlings. Results are presented as relative transcript abundances. The data represent means ± SDs of three replicates.
(c) Cuticular wax composition on rosette leaves and inflorescence stems of Col–0 (WT), *cer26* and *cer26R*. Levels of major components are expressed as µg dm^{-2} of tissue. Each wax constituent is designated by carbon chain length, and is labeled by chemical class along the *x*–axis. The data represent means ± SDs of three replicates.
(d) Stem from a 6–week-old *cer26R* mutant showing a glossy phenotype compared with the wild-type plant stem (Col–0). Epicuticular wax crystal visualization on Arabidopsis wild-type (Col–0) and *cer26R* stem surfaces detected by ESEM at 2800× magnification. Scale bars: 20 µm.

DISCUSSION

CER26 encodes a novel protein involved in wax biosynthesis

As expected for cuticle-associated genes, *CER2*, *CER26* and *CER26-like* expression was found to be restricted to the aerial part of plants. However, the three genes are differentially expressed at the tissue and organ level throughout plant development. *CER2* and *CER26* are highly expressed in leaves, but only *CER2* transcripts were detected in stems. A defect in *CER2* leads to a specific block in the synthesis of wax compounds with more than

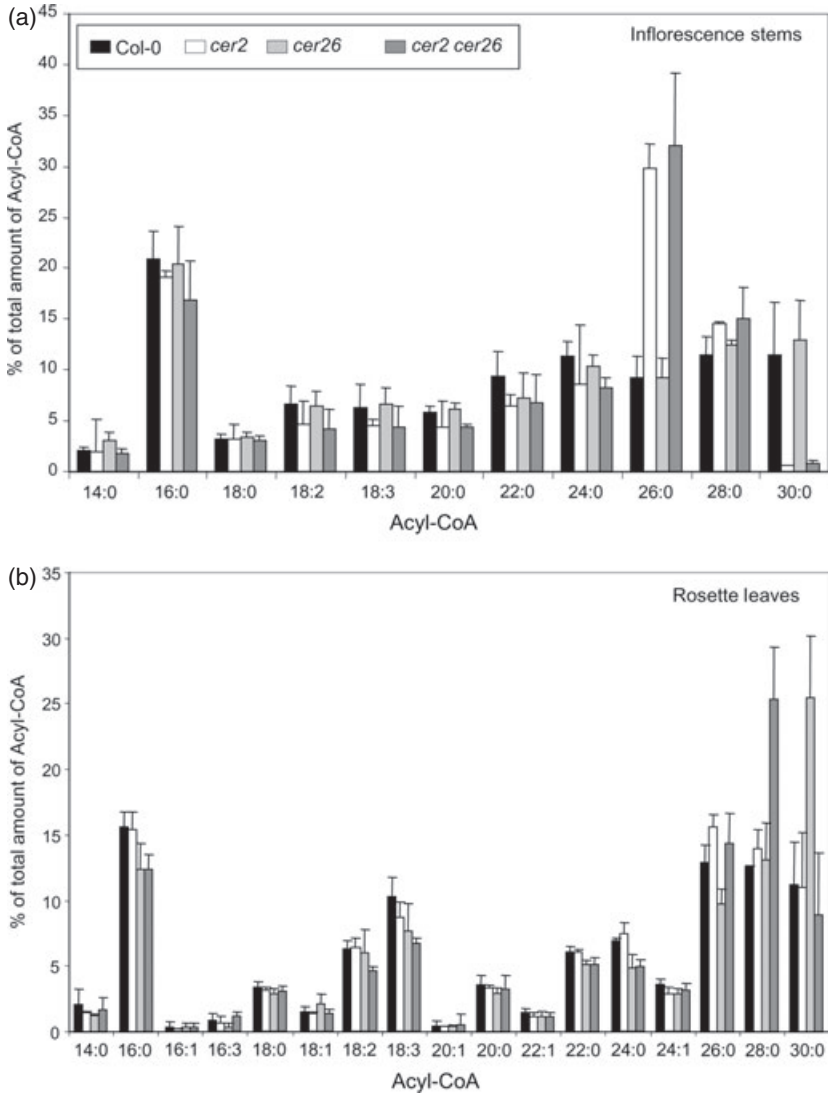

Figure 6. Acyl-CoA profiling of *cer2, cer26* and *cer2 cer26* mutants.
(a) Acyl-CoA profiling of inflorescence stems of Arabidopsis Col–0 (WT), *cer2, cer26* and *cer2 cer26* lines.
(b) Acyl-CoA profiling of rosette leaves of Arabidopsis Col–0 (WT), *cer2, cer26* and *cer2 cer26* lines. Each constituent is designated by carbon chain length along the *x*–axis. Each value represents the mean ± SD of four replicates.

28 carbons in stems. In common with *cer2*, the deregulation of *CER26* affects all classes of wax compounds with a specific carbon chain length pattern, suggesting that CER26 acts on the synthesis of compounds with 30 or more carbons. In accordance with the *CER26* expression pattern, this phenotype was observed in leaves, but not in stems. The involvement of CER26 in the synthesis of wax compounds with more than 30 carbons was further confirmed by the restoration of correct wax biosynthesis in plants overexpressing *CER26* in the *cer26* mutant background. Furthermore, ectopic expression of *CER26* in stems shifts the stem wax composition to a leaf wax composition, further demonstrating that CER26 is implicated in the formation of wax compounds with more than C30 carbons. The *cer26R* line displays a shiny stem phenotype because of the disappearance of the typical crystalline microstructure normally found at the stem surface (Jenks *et al.*, 2002). Little is known about the specific contribution of each of the wax compounds in the formation of wax crystals (Shepherd and Wynne Griffiths, 2006); however, the results presented in this study suggest that a tight balance in the alkane chain length is required for the correct microstructure of waxes.

As mentioned above, our results showed that the *cer2* mutation does not impact wax biosynthesis in leaves, even though *CER2* is expressed in all vegetative organs. Because *CER2* and *CER26* are both expressed in leaves, we hypothesized that CER26 could compensate for the loss of CER2 function in that tissue. Analyses of the *cer2 cer26* mutant confirmed this hypothesis. The double *cer2 cer26*

mutant showed a leaf wax profile different from those of the single *cer2* or *cer26* mutants, indicating that CER2 and CER26 have overlapping functions in the synthesis of wax compounds with more than 28 carbons in leaves.

CER26 and *CER2* inactivation specifically affects VLCFA-containing lipids

As the *cer2* and *cer26* phenotypes suggested that the corresponding proteins are involved in VLCFA elongation, the impact of a defect of CER2 and CER26 was also investigated in all other classes of VLFCA-containing lipids, i.e. cutin, suberin, TAGs and total intracellular fatty acyl chains. In all the lipid pools analyzed, no modification was observed on fatty acyl chains shorter than 26 carbons. In plants cells, VLCFAs with more than 26 carbons can be detected as trace levels in cutin; however, no significant modification of the composition of cutin was observed. VLCFAs can also be detected as trace levels in the total fatty acyl pool. Interestingly, the inactivation of *CER26* and/or *CER2* led to slight modifications of the total fatty acyl profile, in accordance with what was observed in waxes, indicating that CER2 and CER26 act specifically on the elongation of VLCFAs with more than 26 carbons.

CER26 and *CER2* are critical components of the VLCFA elongation process

The global lipid analyses of the *cer2*, *cer26* and *cer2 cer26* mutants performed in our study indicated that CER2 and CER26 are likely to be involved in the formation of fatty acids with a specific chain-length pattern. Subsequent analysis of the acyl-CoA pools in the different mutant lines showed a pattern consistent with that observed in both waxes and intracellular fatty acyl chain composition. As observed in waxes, the block of C28 acyl-CoA elongation in the *cer2* mutant is illustrated by a near disappearance of acyl-CoAs longer than 30 carbons, yet the C28 species are not over-accumulated. Conversely, the level of C26 species is largely increased, suggesting that CER2 could also have an impact on the elongation of C26 acyl-CoA to C28 acyl-CoA. Similarly, CER26, which has a clear role in the elongation of C30 acyl-CoA, is also likely to have a role in the elongation of C32 acyl-CoA because compounds with more than 32 carbons were found to be over-accumulated in stems ectopically expressing *CER26*. Unfortunately, this hypothesis could not be confirmed given the technical limitations of the current methods for acyl-CoA analysis, preventing the accurate detection of species longer than C30.

Towards the functional characterization of CER26

Based on the *cer2* phenotype, a role of CER2 as a stem-specific element of the VLCFA elongase was proposed (Jenks *et al.*, 1995; Negruk *et al.*, 1996; Xia *et al.*, 1996). We showed that CER2, together with the newly identified CER26 protein, is also involved in the elongation of VLCFAs in leaves. Nevertheless, the function of both proteins remains elusive. The combined analysis of wax and acyl-CoA pools in the different mutants showed that *cer2* and *cer26* have phenotypes similar to the KCS mutants. It would therefore be appealing to suggest that both CER2 and CER26 could encode condensing enzymes specific for the elongation of VLCFAs involved in wax biosynthesis. Nevertheless, the CER2-like proteins do not share sequence similarities with the Arabidopsis FAE1-like type of KCSs or the ELO-type of KCSs found in both Arabidopsis and yeast (Yu *et al.*, 2009). Therefore, it is highly unlikely that CER2 and CER26 act as condensing enzymes. Alternatively, CER2 and CER26 could act as regulators of the activity of the elongase complexes generating VLCFAs. As such, they could facilitate the formation of VLC acyl-CoAs by stabilizing the FAE complexes, enhancing their activity or allowing the newly elongated acyl-CoA to be presented back to the KCS enzyme after an elongation cycle. These hypotheses suggest that CER2 and CER26 would be associated with ER membranes. However, CER2-like proteins are members of the BAHD superfamily of acyl-CoA-dependent acyltransferases, which are predicted to be soluble cytosolic enzymes (Yu *et al.*, 2009), of which several have been experimentally shown to localize into the cytosol (Panikashvili *et al.*, 2009; Rautengarten *et al.*, 2012). Analyses of the primary sequences of the CER2-like proteins using prediction tools did not reveal any transmembrane domains, specific targeting signals or post-translational lipid modifications. CER2 was previously localized exclusively in the nucleus, based on immunodetection using subcellular fractions, which would be consistent with the early hypothesis of its regulatory role in the elongation process (Xia *et al.*, 1997), but this does not fit with CER2 annotation as a cytosolic protein. GLOSSY2, the ortholog of CER2 from *Zea mays* (maize), was immunodetected in the cytoplasm fraction, and in a membrane fraction enriched with endoplasmic reticulum (ER) and mitochondria, suggesting that CER2 may be a cytosolic protein recruited to the ER for its activity (Velasco *et al.*, 2002). This study is supported by the work of Haslam and co-workers who have shown, using a *cer2* mutant functionally complemented with a CER2-GFP fusion protein, that CER2 is localized to ER membranes in young epidermal cells at the apex of Arabidopsis stems (Haslam *et al.*, 2012). Similarly, we generated a *cer26* mutant functionally complemented with a YFP-CER26 fusion protein. Unfortunately, although transgenic plants with a normal wax phenotype were obtained and the fusion protein was detected in leaf extract by western blot using an antibody against the YFP, we were not able to localize the protein elsewhere other than in the cytosol of epidermal cells (Figure S7). We hypothesize that, because the CER2 association with the ER was only observed in the epidermal cells of the stem apex (the active site of wax synthesis components), the targeting of

CER2-like proteins to ER membranes potentially requires interaction with microsomal proteins involved in VLCFA elongation. As the production of waxes in leaves is 10 times less important than in stems, the level of proteins involved in the elongation of C30 and C32 VLCFAs, which are potential targets of CER26, could be not sufficient to allow the targeting of the overexpressed CER26 protein to ER membranes that might be visualized using confocal microscopy. In such a model the tight control of CER26 overexpression at the tissue and the cellular level would be necessary to allow the correct localization of the protein. Further investigation must be performed to better understand this mechanism, and protein–protein interaction analysis might provide conclusive evidence that the ER localization of CER26 requires interaction with wax-associated membrane proteins, and notably, members of the FAE complexes.

Little is known about the regulation of elongase complexes throughout kingdoms. To date, the Arabidopsis PAS1 protein is the only example of an FAE complex regulator (Roudier *et al.*, 2010). Similar to a loss of one of the elongase core components, a defect in PAS1 was shown to reduce all VLCFAs in TAGs and sphingolipids. PAS1 is a member of the immunophilin family of chaperones that are known to target protein complexes and regulate their assembly or activity. Although the phenotype of *cer2* and *cer26* shows some similarities with the phenotype of *pas1*, it is not likely that the proteins perform the same function. Indeed, the primary protein structure of CER2 and CER26 does not share similarities with PAS1. Moreover, the *cer2* and *cer26* mutants are only affected in VCLFAs with more than 26 carbons, showing that unlike PAS1, CER2 and CER26 are not involved in the regulation of all FAE complexes.

CER2 and CER26, together with CER26-like, have been annotated as BAHD acyltransferases (Yu *et al.*, 2009), which are characterized by the presence of a conserved catalytic HXXXDG motif near the center position of the enzymes, and a second highly conserved structural C–terminal DFGWG motif. CER2 and CER26 proteins perform similar functions in the elongation process. Nevertheless, the HXXXDG motif was found to be conserved in CER2, but not in CER26, which contains a divergent NXXXDG motif, and neither CER26 nor CER2 contain the DFGWG motif, thus strongly questioning their putative function as acyltransferases. This hypothesis was recently confirmed by functional complementation of the *cer2* mutant phenotype with mutated forms of CER2, in which the histidine residue of the HXXXDG motif was replaced by an alanine or an asparagine, demonstrating that this motif is not essential for the activity of the protein, and suggesting that CER2-like proteins could have a distinct biochemical function (Haslam *et al.*, 2012).

As mentioned above, even though wax biosynthesis has been extensively studied, no KCS enzymes involved in the elongation of acyl chains longer than 30 carbons have been identified so far. In particular, yeast heterologous expression of CER6 was found to produce only C28 fatty acids (Haslam *et al.*, 2012; Tresch *et al.*, 2012), whereas expression of its close homologue CER60 led to the formation of C28 and C30 fatty acids (Trenkamp *et al.*, 2004). This indicates that CER2 and CER26 are not strictly required for the activity of plant KCSs. This idea is further supported by the fact that the production of VLCFAs is not totally abolished in the *cer2 cer26* double mutant. Nevertheless, the expression of CER60 produces only traces of C30, suggesting that the activity of this enzyme is not optimal in these conditions (Trenkamp *et al.*, 2004). Therefore, we hypothesize that the function of CER2 and CER26 is to facilitate the activity of the KCSs specific for VLCFA formation. This hypothesis is supported by recent findings that show that co-expression of CER6 and CER2 in yeast led to the formation of C30 fatty acids (Haslam *et al.*, 2012). In this context, the systematic co-expression of CER26 with plant KCSs in yeast should allow the identification of the KCS(s) enzyme(s) involved in the synthesis of VLCFAs with more than 30 carbons used as wax precursors.

EXPERIMENTAL PROCEDURES

Plant material and growth conditions

Arabidopsis thaliana (L.) Heynh (ecotype Columbia–0) was used in all experiments. The following T–DNA insertion lines were obtained from the Arabidopsis Biological Resource Center (http://www.arabidopsis.org): SALK_084443 (*cer2*), SAIL_3_F11 (*cer26-like*) and SALK_087857 (*cer26*). Arabidopsis plants were grown under controlled conditions, as previously described (Joubès *et al.*, 2008). Measurements of leaf growth variables in control and soil water deficit conditions were performed with the PHENOPSIS automated platform, as previously described (Bourdenx *et al.*, 2011).

DNA, RNA, cDNA preparation, real-time RT-PCR conditions and analysis

Genomic DNA was extracted from Arabidopsis leaves with the DNeasy Plant kit (Qiagen, http://www.qiagen.com) and RNA from Arabidopsis tissues with the RNeasy Plant mini kit (Qiagen). Purified RNA was treated with DNase I using the DNA-free kit (Ambion, now Invitrogen, http://www.invitrogen.com). First-strand cDNA was prepared from 1 μg of total RNA with the Superscript RT II kit (Invitrogen) and oligo$(dT)_{18}$, according to the manufacturer's instructions. A 0.2–μl aliquot of the total reaction volume (20 μl) was used as a template in real-time RT-PCR amplification. The PCR amplification was performed with the gene-specific primers listed in Table S2. PCR efficiency ranged from 95 to 105%. All samples were assayed in triplicate wells. Real-time PCR was performed on iCycler (Bio-Rad, http://www.bio-rad.com). Samples were amplified in a 25–μl reaction containing 1x SYBR Green Master Mix (Bio-Rad) and 300 nM of each primer. The thermal profile consisted of one cycle at 95°C for 3 min and 30 s, followed by 40 cycles at 95°C for 30 s and at 58°C for 30 s. For each run, data acquisition and analysis was performed using iCycler iQ 3.0 a (Bio-Rad). The transcript abundance in samples was determined using

a comparative cycle threshold (C_t) method. The relative abundance of *ACT2, EF–1α, eIF-4A–1, UBQ10 and PP2A* mRNAs (Czechowski *et al.*, 2005) in each sample was determined and used to normalize for differences of total RNA level according to the method described by Vandesompele *et al.* (2002). Semiquantitative RT-PCR analysis and PCR on genomic DNA were performed using Phire Hot Start DNA Polymerase (Finnzymes, http://diagnostics.finnzymes.fi).

Cloning and transgenic plants

Promoter sequences and open reading frames (ORFs) were amplified from Arabidopsis genomic DNA and from cDNA, respectively, using the primers listed in Table S2. The corresponding PCR fragments were cloned into the pDONR221 ENTRY vector by GATEWAY® recombinational cloning technology, and subsequently transferred into the pKGWFS7, pK7WG2D and pH7WGY2 DESTINATION vectors (Karimi *et al.*, 2002) by LR cloning. Constructs transferred into the *Agrobacterium tumefaciens* C58C1Rif^R strain harboring the plasmid pMP90 were used to generate stably transformed Arabidopsis plants using the floral-dip transformation method (Clough and Bent, 1998). Histochemical GUS analyses were performed as described by Joubès *et al.* (2008).

Lipid analyses

Cuticular wax analysis. Epicuticular waxes were extracted from leaves and stems by immersing tissues for 30 s in chloroform containing docosane as the internal standard. Extracts were derivatized and analyzed as described by Bourdenx *et al.* (2011). For epicuticular wax crystal formation on Arabidopsis stem surfaces, segments from the apical part of the stem were mounted onto stubs and viewed with an FEI Quanta 200 microscope used in environmental scanning electron microscopy (ESEM) mode.

Analysis of Acyl-CoA composition. Leaf and stem tissues from 5–week-old plants were collected and used for acyl-CoA extraction, as described by Larson and Graham (2001). Profiling was performed as described by Haynes *et al.* (2008).

Analysis of lipid polyester composition (cutin and suberin). Fresh leaf and stem tissues and roots from 5–week-old plants were collected and immersed in hot isopropanol for 10 min at 80°C. After cooling, samples were extensively delipidated by extracting the soluble lipids, then dried and depolymerized as described by Domergue *et al.* (2010). Extraction, derivatization and analysis were performed as described by Domergue *et al.* (2010).

Analysis of total fatty acid composition. Total fatty acid from stems and leaves were transesterified overnight and analyzed as described by Mongrand *et al.* (1997).

Analysis of seed triacylglycerol composition. Seed triacylglycerol composition analysis was performed as described by Katavic *et al.* (1995).

Accession numbers. Sequence data from this article can be found in the Arabidopsis Genome Initiative or GenBank/EMBL databases under the following accession numbers: *CER2*, At4g24510; *CER26*, At4g13840; *CER26-like*, At3g23840; *CER1*, At1g02205; *Actin2*, At1g49240; *eIF4A-1*, At3g13920; *EF-1a*, At5g60390; *UBQ10*, At4g05320; *PP2A*, At1g13320.

ACKNOWLEDGEMENTS

This work was supported by the Ministère de l'Enseignement Supérieur et de la Recherche (doctoral fellowship for AB), by the Centre National de la Recherche Scientifique and the University Bordeaux Segalen, and by the Biotechnology and Biological Sciences Research Council (grant support to Rothamsted Research). We thank the Salk Institute for Genomic Analysis Laboratory and the Arabidopsis Biological Resource Center for providing the sequence-indexed Arabidopsis T–DNA insertion lines. Scanning electron microscopy and confocal microscopy analyses were carried out at Bordeaux Imaging Center (http://www.bic.u-bordeaux2.fr). Lipid analyses were carried out at Metabolome facility of Bordeaux (http://www.cgfb.u-bordeaux2.fr/en/metabolome).

SUPPORTING INFORMATION

Additional Supporting Information may be found in the online version of this article.

Figure S1. Phylogenic analysis of the Arabidopsis BAHD sequences.

Figure S2. Cuticular wax composition of *cer26-like* mutant.

Figure S3. Composition of residual bound lipids in inflorescence stems and rosette leaves of Arabidopsis Col–0 (WT), *cer2*, *cer26* and *cer2 cer26* lines.

Figure S4. Relative suberin composition of the roots of Arabidopsis Col–0 (WT), *cer2*, *cer26* and *cer2 cer26* lines.

Figure S5. Composition of lipids in seeds of Arabidopsis Col–0 (WT), *cer2*, *cer26* and *cer2 cer26* lines.

Figure S6. Total fatty acyl chain composition in inflorescence stems and rosette leaves of Arabidopsis Col–0 (WT), *cer2*, *cer26* and *cer2 cer26* lines.

Figure S7. Study of the subcellular localization of CER26.

Table S1. Phenotypic traits of Arabidopsis Col–0 (WT), *cer2, cer26* and *cer2 cer26* lines.

Table S2. Primers used for PCR cloning and PCR analysis.

REFERENCES

Beisson, k F., Li-Beisson, Y. and Pollard, M. (2012) Solving the puzzles of cutin and suberin polymer biosynthesis. *Curr. Opin. Plant Biol.* **15**, 329–337.

Bernard, A., Domergue, F., Pascal, S., Jetter, R., Renne, C., Faure, J.D., Haslam, R.P., Napier, J.A., Lessire, R. and Joubès, J. (2012) Reconstitution of plant alkane biosynthesis in yeast demonstrates that Arabidopsis ECERIFERUM1 and ECERIFERUM3 are core components of a very-long-chain-alkane synthesis complex. *Plant Cell*, **24**, 3106–3118.

Bourdenx, B., Bernard, A., Domergue, F. *et al.* (2011) Overexpression of Arabidopsis *ECERIFERUM1* promotes wax VLC-alkane biosynthesis and influences plant response to biotic and abiotic stresses. *Plant Physiol.* **156**, 29–45.

Buschhaus, C. and Jetter, R. (2011) Composition differences between epicuticular and intracuticular wax substructures: how do plants seal their epidermal surfaces? *J. Exp. Bot.* **62**, 841–853.

Clough, S.J. and Bent, A.F. (1998) Floral dip: a simplified method for Agrobacterium-mediated transformation of *Arabidopsis thaliana*. *Plant J.* **16**, 735–743.

Czechowski, T., Stitt, M., Altmann, T., Udvardi, M.K. and Scheible, W.R. (2005) Genome-wide identification and testing of superior reference genes for transcript normalization in *Arabidopsis*. *Plant Physiol.* **139**, 5–17.

Domergue, F., Vishwanath, S.J., Joubes, J. *et al.* (2010) Three *Arabidopsis* Fatty Acyl-CoA Reductases, FAR1, FAR4, and FAR5, Generate Primary Fatty Alcohols Associated with Suberin Deposition. *Plant Physiol.* **153**, 1539–1554.

Dominguez, E., Heredia-Guerrero, J.A. and Heredia, A. (2011) The biophysical design of plant cuticles: an overview. *New Phytol.* **189**, 938–949.

Eigenbrode, S.D., Rayor, L., Chow, J. and Latty, P. (2000) Effects of wax bloom variation in *Brassica oleracea* on foraging by a vespid wasp. *Entomol. Exp. Appl.* **97**, 161–166.

Fiebig, A., Mayfield, J.A., Miley, N.L., Chau, S., Fischer, R.L. and Preuss, D. (2000) Alterations in *CER6*, a gene identical to *CUT1*, differentially affect long-chain lipid content on the surface of pollen and stems. *Plant Cell*, **12**, 2001–2008.

Goodwin, S.M., Chen, X., Rahman, M., Krochko, J. and Jenks, M.A. (2004) ECERIFERUM25 represents a new locus associated with both cutin and cuticular wax production in Arabidopsis. ASPB Annual Meeting.

Granier, C., Aguirrezabal, L., Chenu, K. *et al.* (2006) PHENOPSIS, an automated platform for reproducible phenotyping of plant responses to soil water deficit in *Arabidopsis thaliana* permitted the identification of an accession with low sensitivity to soil water deficit. *New Phytol.* **169**, 623–635.

Gray, J.E., Holroyd, G.H., van der Lee, F.M., Bahrami, A.R., Sijmons, P.C., Woodward, F.I., Schuch, W. and Hetherington, A.M. (2000) The HIC signalling pathway links CO_2 perception to stomatal development. *Nature*, **408**, 713–716.

Greer, S., Wen, M., Bird, D., Wu, X., Samuels, L., Kunst, L. and Jetter, R. (2007) The cytochrome P450 enzyme CYP96A15 is the midchain alkane hydroxylase responsible for formation of secondary alcohols and ketones in stem cuticular wax of *Arabidopsis*. *Plant Physiol.* **145**, 653–667.

Hannoufa, A., McNevin, J. and Lemieux, B. (1993) Epicuticular waxes of *eceriferum* mutants of *Arabidopsis thaliana*. *Phytochemistry* **33**, 851–855.

Haslam, T.M., Mañas Fernández, A., Zhao, L. and Kunst, L. (2012) Arabidopsis ECERIFERUM2 is a component of the fatty acid elongation machinery required for fatty acid extension to exceptional lengths. *Plant Physiol.* **160**, 1164–1174.

Haynes, C.A., Allegood, J.C., Sims, K., Wang, E.W., Sullards, M.C. and Merrill, A.H. Jr (2008) Quantitation of fatty acyl-coenzyme As in mammalian cells by liquid chromatography-electrospray ionization tandem mass spectrometry. *J. Lipid. Res.* **49**, 1113–1125.

Jenks, M.A., Tuttle, H.A., Eigenbrode, S.D. and Feldmann, K.A. (1995) Leaf Epicuticular Waxes of the *Eceriferum* Mutants in *Arabidopsis*. *Plant Physiol.* **108**, 369–377.

Jenks, M.A., Eigenbrode, S.D. and Lemieux, B. (2002) Cuticular waxes of Arabidopsis. In *The Arabidopsis Book*. (Somerville C.R., Meyerowitz M.E., eds). American Society of Plant Biologists, 1:e0016.

Joubès, J., Raffaele, S., Bourdenx, B., Garcia, C., Laroche-Traineau, J., Moreau, P., Domergue, F. and Lessire, R. (2008) The VLCFA elongase gene family in *Arabidopsis thaliana*: phylogenetic analysis, 3D modelling and expression profiling. *Plant Mol. Biol.* **67**, 547–566.

Karimi, M., Inze, D. and Depicker, A. (2002) GATEWAY vectors for *Agrobacterium*-mediated plant transformation. *Trends Plant Sci.* **7**, 193–195.

Katavic, V., Reed, D.W., Taylor, D.C., Giblin, E.M., Barton, D.L., Zou, J., Mackenzie, S.L., Covello, P.S. and Kunst, L. (1995) Alteration of seed fatty acid composition by an ethyl methanesulfonate-induced mutation in Arabidopsis thaliana affecting diacylglycerol acyltransferase activity. *Plant Physiol.* **108**, 399–409.

Koornneef, M., Hanhart, C.J. and Thiel, F. (1989) A genetic and phenotypic description of *Eceriferum* (*cer*) mutants in *Arabidopsis thaliana*. *J. Hered.* **80**, 118–122.

Kosma, D.K., Bourdenx, B., Bernard, A., Parsons, E.P., Lu, S., Joubes, J. and Jenks, M.A. (2009) The impact of water deficiency on leaf cuticle lipids of *Arabidopsis*. *Plant Physiol.* **151**, 1918–1929.

Kunst, L. and Samuels, A.L. (2003) Biosynthesis and secretion of plant cuticular wax. *Prog. Lipid Res.* **42**, 51–80.

Kunst, L. and Samuels, L. (2009) Plant cuticles shine: advances in wax biosynthesis and export. *Curr. Opin. Plant Biol.* **12**, 721–727.

Larson, T.R. and Graham, I.A. (2001) Technical Advance: a novel technique for the sensitive quantification of acyl CoA esters from plant tissues. *Plant J.* **25**, 115–125.

Li, F., Wu, X., Lam, P., Bird, D., Zheng, H., Samuels, L., Jetter, R. and Kunst, L. (2008) Identification of the wax ester synthase/acyl-coenzyme A: diacylglycerol acyltransferase WSD1 required for stem wax ester biosynthesis in *Arabidopsis*. *Plant Physiol.* **148**, 97–107.

McNevin, J.P., Woodward, W., Hannoufa, A., Feldmann, K.A. and Lemieux, B. (1993) Isolation and characterization of *eceriferum* (*cer*) mutants induced by T-DNA insertions in *Arabidopsis thaliana*. *Genome*, **36**, 610–618.

Millar, A.A., Clemens, S., Zachgo, S., Giblin, E.M., Taylor, D.C. and Kunst, L. (1999) CUT1, an Arabidopsis gene required for cuticular wax biosynthesis and pollen fertility, encodes a very-long-chain fatty acid condensing enzyme. *Plant Cell*, **11**, 825–838.

Mongrand, S., Bessoule, J.J. and Cassagne, C. (1997) A re-examination *in vivo* of the phosphatidylcholine-galactolipid metabolic relationship during plant lipid biosynthesis. *Biochem J.* **327**, 853–858.

Negruk, V., Yang, P., Subramanian, M., McNevin, J.P. and Lemieux, B. (1996) Molecular cloning and characterization of the *CER2* gene of *Arabidopsis thaliana*. *Plant J.* **9**, 137–145.

Panikashvili, D., Shi, J.X., Schreiber, L. and Aharoni, A. (2009) The Arabidopsis *DCR* encoding a soluble BAHD acyltransferase is required for cutin polyester formation and seed hydration properties. *Plant Physiol.* **151**, 1773–1789.

Pruitt, R.E., Vielle-Calzada, J.P., Ploense, S.E., Grossniklaus, U. and Lolle, S.J. (2000) *FIDDLEHEAD*, a gene required to suppress epidermal cell interactions in Arabidopsis, encodes a putative lipid biosynthetic enzyme. *Proc. Natl Acad. Sci. USA*, **97**, 1311–1316.

Raffaele, S., Leger, A. and Roby, D. (2009) Very long chain fatty acid and lipid signaling in the response of plants to pathogens. *Plant Signal. Behav.* **4**, 94–99.

Rashotte, A., Jenks, M., Ross, A. and Feldmann, K. (2004) Novel *eceriferum* mutants in *Arabidopsis thaliana*. *Planta* **219**, 5–13.

Rautengarten, C., Ebert, B., Ouellet, M. *et al.* (2012) Arabidopsis *deficient in cutin ferulate* encodes a transferase required for feruloylation of ω-hydroxy fatty acids in cutin polyester. *Plant Physiol.* **158**, 654–665.

Roudier, F., Gissot, L., Beaudoin, F. *et al.* (2010) Very long chain fatty acids are involved in polar auxin transport and developmental patterning in Arabidopsis. *Plant Cell*, **22**, 364–375.

Rowland, O., Zheng, H., Hepworth, S.R., Lam, P., Jetter, R. and Kunst, L. (2006) *CER4* encodes an alcohol-forming fatty acyl-coenzyme A reductase involved in cuticular wax production in *Arabidopsis*. *Plant Physiol.* **142**, 866–877.

Shepherd, T. and Wynne Griffiths, D. (2006) The effects of stress on plant cuticular waxes. *New Phytol.* **171**, 469–499.

Todd, J., Post-Beittenmiller, D. and Jaworski, J.G. (1999) KCS1 encodes a fatty acid elongase 3-ketoacyl-CoA synthase affecting wax biosynthesis in *Arabidopsis thaliana*. *Plant J.* **17**, 119–130.

Trenkamp, S., Martin, W. and Tietjen, K. (2004) Specific and differential inhibition of very-long-chain fatty acid elongases from Arabidopsis thaliana by different herbicides. *Proc. Natl Acad. Sci. USA*, **101**, 11903–11908.

Tresch, S., Heilmann, M., Christiansen, N., Looser, R. and Grossmann, K. (2012) Inhibition of saturated very-long-chain fatty acid biosynthesis by mefluidide and perfluidone, selective inhibitors of 3-ketoacyl-CoA synthases. *Phytochemistry* **76**, 162–171.

Vandesompele, J., De Preter, K., Pattyn, F., Poppe, B., Van Roy, N., De Paepe, A. and Speleman, F. (2002) Accurate normalization of real-time quantitative RT-PCR data by geometric averaging of multiple internal control genes. *Genome Biol.* **3**, 1–11.

Velasco, R., Korfhage, C., Salamini, A., Tacke, E., Schmitz, J., Motto, M., Salamini, F. and Döring, H.-P. (2002) Expression of the *glossy2* gene of maize during plant development. *Maydica*, **47**, 71–81.

von Wettstein-Knowles, P. (1982) Elongase and epicuticular wax biosynthesis. *Physiol Vég.* **20**, 797–809.

Xia, Y., Nikolau, B.J. and Schnable, P.S. (1996) Cloning and characterization of *CER2*, an Arabidopsis gene that affects cuticular wax accumulation. *Plant Cell*, **8**, 1291–1304.

Xia, Y., Nikolau, B.J. and Schnable, P. (1997) Developmental and hormonal regulation of the Arabidopsis *CER2* gene that codes for a nuclear-localized protein required for the normal accumulation of cuticular waxes. *Plant Physiol.* **115**, 925–937.

Yephremov, A., Wisman, E., Huijser, P., Huijser, C., Wellesen, K. and Saedler, H. (1999) Characterization of the FIDDLEHEAD gene of Arabidopsis reveals a link between adhesion response and cell differentiation in the epidermis. *Plant Cell*, **11**, 2187–2201.

Yu, X.H., Gou, J.Y. and Liu, C.J. (2009) BAHD superfamily of acyl-CoA dependent acyltransferases in Populus and Arabidopsis: bioinformatics and gene expression. *Plant Mol. Biol.* **70**, 421–442.